

# Source Temperatures and Sizes in Central Collisions

C. Schwarz<sup>(1)</sup> for the ALADIN collaboration:

R. Bassini,<sup>(2)</sup> M. Begemann-Blaich,<sup>(1)</sup> A.S. Botvina,<sup>(3)\*</sup> S. Fritz,<sup>(1)</sup> S.J. Gaff,<sup>(4)</sup>  
C. Groß,<sup>(1)</sup> G. Immé,<sup>(5)</sup> I. Iori,<sup>(2)</sup> U. Kleinevoß,<sup>(1)</sup> G.J. Kunde,<sup>(4)</sup> W.D. Kunze,<sup>(1)</sup>  
U. Lynen,<sup>(1)</sup> V. Maddalena,<sup>(5)</sup> M. Mahi,<sup>(1)</sup> T. Möhlenkamp,<sup>(6)</sup> A. Moroni,<sup>(2)</sup>  
W.F.J. Müller,<sup>(1)</sup> C. Nociforo,<sup>(5)</sup> B. Ocker,<sup>(7)</sup> T. Odeh,<sup>(1)</sup> F. Petruzzelli,<sup>(2)</sup>  
J. Pochodzalla,<sup>(1)†</sup> G. Raciti,<sup>(5)</sup> G. Riccobene,<sup>(5)</sup> F.P. Romano,<sup>(5)</sup> Th. Rubehn,<sup>(1)‡</sup>  
A. Saija,<sup>(5)</sup> M. Schnittker,<sup>(1)</sup> A. Schüttauf,<sup>(7)</sup> W. Seidel,<sup>(6)</sup> V. Serfling,<sup>(1)</sup>  
C. Sfienti,<sup>(5)</sup> W. Trautmann,<sup>(1)</sup> A. Trzcinski,<sup>(8)</sup> G. Verde,<sup>(5)</sup> A. Wörner,<sup>(1)</sup>  
Hongfei Xi,<sup>(1)§</sup> and B. Zwieglinski<sup>(8)</sup>

<sup>(1)</sup>Gesellschaft für Schwerionenforschung, D-64291 Darmstadt, Germany

<sup>(2)</sup>Istituto di Scienze Fisiche dell' Università and I.N.F.N., I-20133 Milano, Italy

<sup>(3)</sup>Institute for Nuclear Research, Russian Academy of Sciences, 117312 Moscow ,  
Russia

<sup>(4)</sup>Department of Physics and Astronomy and National Superconducting Cyclotron  
Laboratory, Michigan State University, East Lansing, MI 48824, USA

<sup>(5)</sup>Dipartimento di Fisica dell' Università and I.N.F.N., I-95129 Catania, Italy

<sup>(6)</sup>Forschungszentrum Rossendorf, D-01314 Dresden, Germany

<sup>(7)</sup>Institut für Kernphysik, Universität Frankfurt, D-60486 Frankfurt, Germany

<sup>(8)</sup>Soltan Institute for Nuclear Studies, 00-681 Warsaw, Hoza 69, Poland

## ABSTRACT

For midrapidity fragments from central 50-200 A MeV Au+Au collisions temperatures from double ratios of isotopic yields were compared with temperatures from particle unbound states. Temperatures from particle unbound states with  $T \simeq 4-5 \text{ MeV}$  show with increasing beam energy an increasing difference to temperatures from double ratios of isotopic yields, which increase from  $T \simeq 5 \text{ MeV}$  to  $T \simeq 12 \text{ MeV}$ . The lower temperatures extracted from particle unstable states can be explained by increasing cooling of the decaying system due to expansion. This expansion is driven by the radial flow, and freeze out of particle unstable states might depend on the

---

\* Present Address: Bereich Theoretische Physik, Hahn-Meitner-Institut, D-14109 Berlin, Germany

† Present address: Max-Planck-Institut für Kernphysik, D-69117 Heidelberg, Germany

‡ Present address: Nuclear Science Division, Lawrence Berkeley Laboratory, Berkeley, CA 94720, USA

§ Present address: NSCL, Michigan State University, East Lansing, MI 48824, USA

dynamics of the expanding system. Source sizes from pp-correlation functions were found to be 9 to 11 fm.

Highly excited nuclear matter with excitation energies above the binding energy is formed in collisions between heavy nuclei. Projectile spectators from 600 A MeV Au + Au collisions [1, 2, 3] show with increasing excitation energy per nucleon after a temperature rise according to a Fermi liquid a temperature plateau of about  $T \simeq 5$  MeV (Fig. 1). Farther excitation shows up as a linear temperature increase in accordance with a gas of free nucleons. This relation commonly referred to as caloric curve was interpreted by the authors as reminiscent of a nuclear liquid-gas phase transition [1]. The above temperatures were deduced from double ratios of isotopic

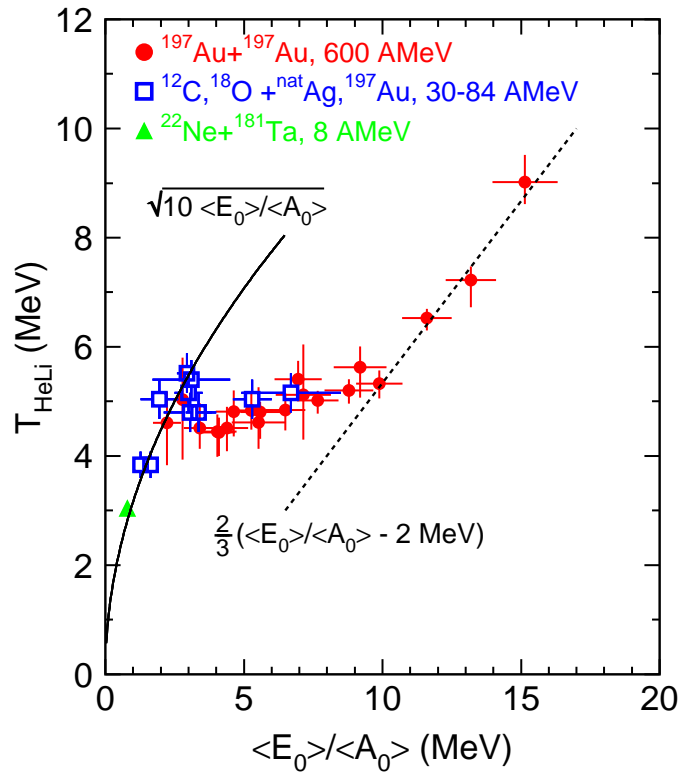


Figure 1: Caloric curve from Ref. [1]

fragment yields [4]. The underlying assumptions of thermal and chemical equilibrium for the mass action law for this temperature measurement are also questioned taking into account interaction between particles leading to Mott transitions [5]. The following debate about the order of the phase transition gained a great deal by alternative interpretations like sequential feeding [6, 7] and Coulomb instabilities [8] of systems, where the mass decreases with the excitation energies. It is therefore of interest to

extract the caloric curve of participant matter with nearly constant mass and increasing excitation energy. To shed light on this problems it is helpful to compare the chemical temperatures with temperatures deduced from the population of particle unstable states which are well established for temperatures up to  $T = 6 \text{ MeV}$  [9, 10]. Therefore, we performed an experiment to measure both temperatures for midrapidity fragments in Au+Au collisions.

The experiment was performed using  $^{197}\text{Au}$  beams of 50, 100, 150, and 200 AMeV, respectively, extracted from the heavy-ion synchrotron SIS of the GSI facility:

Targets with areal densities of  $75 \text{ mg/cm}^2$  were irradiated with beam intensities of  $10^6 \text{ s}^{-1}$ . A set of seven telescopes, shown in Fig. 2 consisting of 50, 300, 1000  $\mu\text{m}$  Si-surface barrier detectors followed by an 4 cm long CsI(Tl) scintillator with photodiode readout were used to measure isotopically resolved fragment spectra.

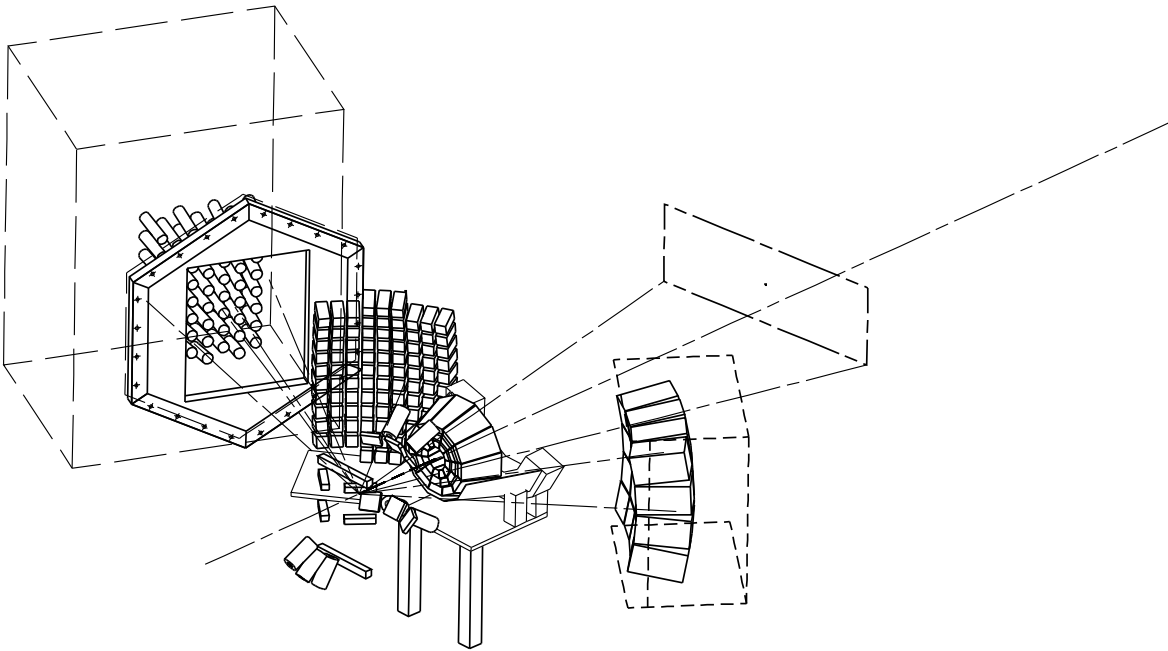


Figure 2: Setup with 3 hodoscopes and the zero degree hodoscope. The beam comes from the left. The GSI hodoscope on the right side and the Catania hodoscope on the left side measured two-particle correlation-functions. On the same side the MSU hodoscope was setup at larger angles. The Zero Degree Outer hodoscope (ZDO) around the beam axis served together with 48 Si-strip detectors at angles,  $\theta \approx 40^\circ$  for the impact parameter selection. Isotopic resolved fragment spectra were measured with 7 telescopes around the target.

Four telescopes measured at  $\theta_{lab} = 40^\circ$  particle yields from the midrapidity source, the other telescopes were located at  $\theta_{lab} = 110^\circ$ ,  $130^\circ$ , and  $150^\circ$ . Permanent magnets, placed next to the entrance collimator of each telescope, deflected electrons produced in the target. Isotopic resolution was achieved up to carbon fragments; the energy thresholds for p, d, t,  $^3\text{He}$ ,  $^4\text{He}$ ,  $^6\text{Li}$ ,  $^7\text{Li}$  were 2.1, 2.7, 3.1, 6.8, 7.4, 13.9, and 14.4 AMeV, respectively. Three hodoscopes built at GSI, LNS Catania, and Michigan State University and consisting, in total, of 216 Si-CsI(Tl) telescopes were setup at distances between 0.6 m and 1.1 m from the target. The GSI hodoscope which consisted of 64 elements and the Catania hodoscope which consisted of 96 elements covered an angular range between  $\theta_{lab} = 24^\circ - 59^\circ$ . The correlation data obtained with these two hodoscopes and the telescopes are the subject of this paper and consist of an  $300 \mu\text{m}$  Si-detector followed by a 6 cm long CsI(Tl) scintillator with photodiode readout. For the Catania hodoscope, each telescope had a solid angle of  $= 2.95 \text{ msr}$ , and the angular spacing between adjacent telescopes was  $\Delta\theta = 0.22^\circ$ . For the GSI hodoscopes, each 4 detectors were combined in a group with an angular spacing of  $\Delta\theta < 0.01^\circ$  within and  $\Delta\theta = 2.5^\circ$  between the groups of detectors. The covered solid angle of each detector was  $\Delta\Omega = 1.35 \text{ msr}$ . Energy calibration

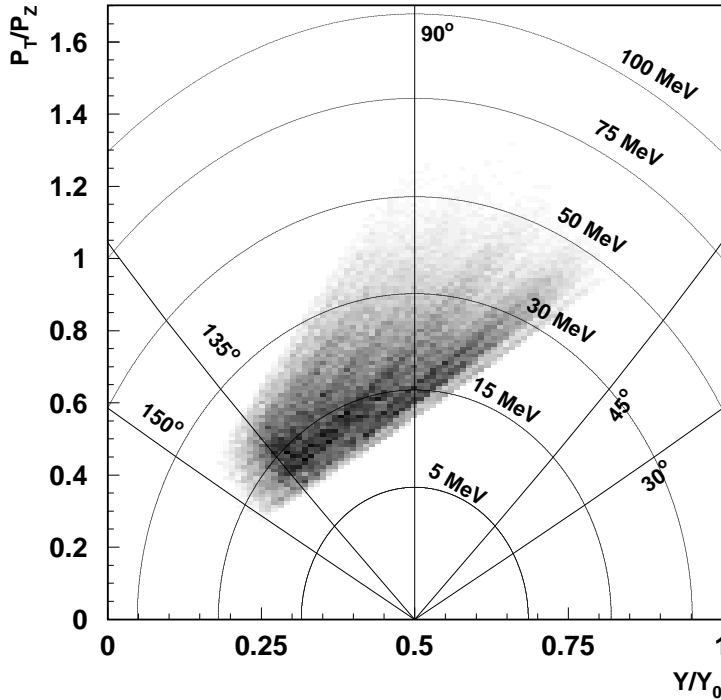


Figure 3: Acceptance of the hodoscopes for detected p- $\alpha$  pairs at 150 AMeV beam energy. At all incident energies the fragments were detected at  $\theta_{CMS} \approx 90^\circ$ .

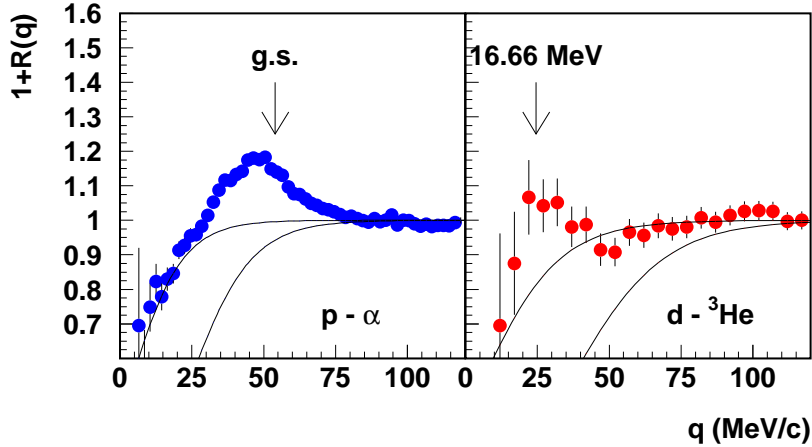


Figure 4: Correlation functions coincident  $p$ - $\alpha$  pairs (left panel) and  $d$ - ${}^3\text{He}$  pairs (right panel) at 150 A MeV beam energy. The lines denote extrem assumptions about the background correlation function which were guided by scaled correlation functions of nonresonant states. The nonresonant correlation functions were assumed to scale with the relative velocity between the pairs. with

for individual detectors of the hodoscopes were obtained by employing energies of fragments just stopped in the dE-Silicon counters and the CsI(Tl) crystals. This resulted in calibrations with accuracies of about 2 % for protons and 3 % for Lithium. These calibration accuracies were assessed by comparing peak widths of experimental and calculated correlation functions. In addition, 36 phoswich detectors and 48 Si-strip detectors from  $6.5^\circ$  to  $40^\circ$  increased the solid angle and the granularity of the detector system and allowed impact parameter selection.

The angular range of our hodoscopes were chosen around  $\theta_{cm} = 90^\circ$  in order to minimize contributions from target like and projectile like sources. The acceptance for the GSI and the Catania hodoscope is shown in Fig. 3 for  ${}^5\text{Li}$ , reconstructed from coincident measured proton-alpha pairs. Charged particle multiplicities served as impact parameter filter, and we selected the most central collisions (9% of yield) in accordance with an reduced impact parameter range of  $\hat{b} = 0.3$ .

We employed correlation functions in order to determine temperatures from particle unstable states. For the extraction of the yields we assumed two extreme assumptions of the background correlation function which determine our systematical errors. They were constructed with the help of the correlation functions from fragments without resonant states. For technical details of the extraction of the temperatures see Ref. [9]. We also used the decay of  ${}^8\text{Be}$  as thermometer, the results for all incident energies are shown in Tab. 1. They all agree with an average apparent temperature

$E_{Beam}$ (AMeV)	$T_{excited}$ (MeV)	$T_{double\ rat.}$ (MeV)		
50MeV/A	${}^5Li$	$4.2^{+1.2}_{-0.3}$	$({}^6Li/{}^7Li)/({}^3He/{}^4He)$	$5.3 \pm 0.8$
	${}^8Be$	$5.0^{+2.6}_{-0.6}$	$({}^6Li/{}^7Li)/({}^2H/{}^3H)$	$4.7 \pm 0.5$
100MeV/A	${}^5Li$	$3.7^{+2.3}_{-0.6}$	$({}^6Li/{}^7Li)/({}^3He/{}^4He)$	$8.9 \pm 0.1$
	${}^8Be$	$4.3^{+2.6}_{-0.5}$	$({}^6Li/{}^7Li)/({}^2H/{}^3H)$	$7.0 \pm 0.1$
150MeV/A	${}^5Li$	$3.9^{+2.1}_{-0.4}$	$({}^6Li/{}^7Li)/({}^3He/{}^4He)$	$10.3 \pm 0.4$
	${}^8Be$	$5.1^{+3.0}_{-0.6}$	$({}^6Li/{}^7Li)/({}^2H/{}^3H)$	$8.2 \pm 0.2$
200MeV/A	${}^5Li$	$3.9^{+2.2}_{-0.3}$	$({}^6Li/{}^7Li)/({}^3He/{}^4He)$	$11.9 \pm 0.4$
	${}^8Be$	$5.0^{+3.0}_{-0.6}$	$({}^6Li/{}^7Li)/({}^2H/{}^3H)$	$9.0 \pm 0.4$

Table 1: Temperatures for central collision ( $\hat{b} \leq 0.3$ ) extracted from particle unstable states ( $T_{excited}$ ) and from double ratios of isotopic yields ( $T_{double\ rat.}$ ) with their systematical errors. For statistical reasons no impact parameter cut was applied to the 50 AMeV data

of  $T \approx 4 - 5$  MeV. As an example for the decay of  ${}^5Li$  the correlation function of its decay products is shown in Fig. 4.

Chemical temperatures, extracted from double ratios of  $({}^3He/{}^4He)/({}^6Li/{}^7Li)$  and  $(d/t)/({}^3He/{}^4He)$  [1], for the Si-telescope at a polar angle of  $\theta_{lab} = 40^\circ$ , are shown in Fig. 5 for central collisions. For deuterons and tritons a correction for the limited acceptance of particles traversing through the detector was done with the help of a moving-source parametrization. Low energy thresholds were low enough to observe the maximum in the energy spectra. By estimating the excitation energy of the reaction zone it is possible to compare these temperatures with those of the caloric curve for spectator matter in Fig. 1. Using as excitation energy the maximum possible excitation energy ( $E_{beam}/4$ ) and subtracting the known values of collective motion (radial flow) [14] the four datapoints resemble the second rise in the caloric curve.

It is surprising that with increasing beam energy there is a growing disagreement between chemical temperatures from double ratios of fragment yields and temperatures extracted from particle unbound states. While for 50 AMeV beam energy both temperatures agree within the error bars, the chemical temperatures at 200 AMeV beam energy are higher by a factor of 4 compared to temperatures from excited states. A known effect, the sequential feeding, which alters the measured temperatures, is still under investigation [6, 7]. For the chemical temperatures, however, we have applied a sequential feeding correction of a factor of 1.2 to the temperatures, which we determined from model comparisons [1]. For temperatures from particle unbound states many investigations of sequential feeding were performed (see eg. [11]). Especially, temperatures from  ${}^5Li$  and  ${}^8Be$  were shown to be quite robust against sequential feeding for temperatures  $T < 5MeV$ .

Taking the temperature difference of both thermometers for true, the different

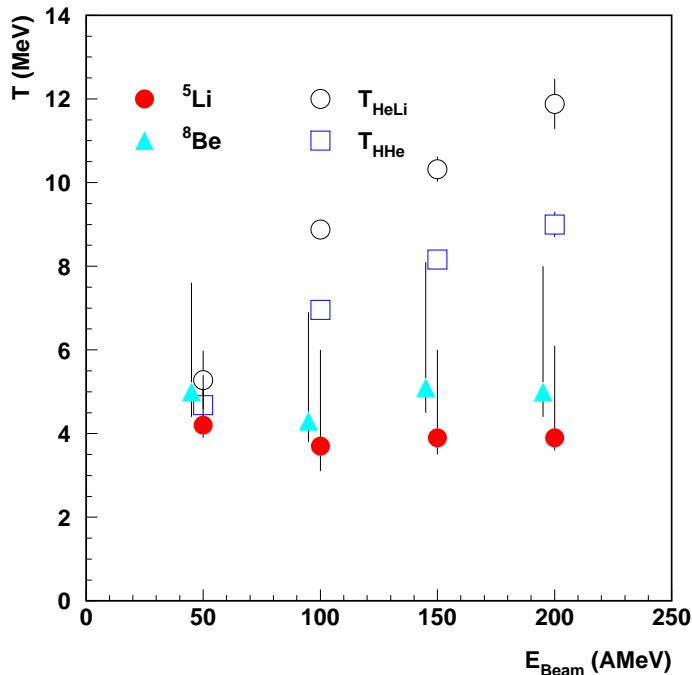


Figure 5: Temperatures from double ratios of isotopic yields (open symbols) compared to temperatures from particle unstable states (closed symbols).

freeze out conditions for both thermometers must be different. In the initial stage of the reaction the density will be high and fragments will not yet have their identity. Below a certain density fragments will be formed and destroyed by the surrounding hot nuclear medium. When the fragments have reached their final identity (chemical equilibrium is achieved), the isotopic ratios reflect temperatures which we have presented in this work. A further step in time order is the formation of excited states. If one assumes that the excited states are quite fragile objects in the surrounding gas of nucleons they will be destroyed and formed later in time as compared to compact particle stable fragments. Therefore, the temperatures from excited states might be lower because of the cooling of the reaction zone. Indeed, NMD calculations [12] show for central Au+Au collisions at 150 AMeV that fragments already formed suffer for time intervals up to 30-50 fm/c collisions with the surrounding environment.

The expanding source scenario that evolves with increasing incident energies also influences the proton-proton correlation function, from which information about the space-time behaviour of the source may be obtained [13]. The correlation functions for proton pairs from reactions at 100, 150, and 200 AMeV incident energies are shown in Fig. 6 (data points). From QSM [15] calculations, with parameters selected to



describe measured yields, the fractions of protons emitted from long lived resonances were estimated to be 0.21, 0.29, and 0.31 for 100, 150, and 200 AMeV, respectively. The data were corrected for this effect and source sizes were deduced by comparing these correlation functions with predictions of the Koonin-Pratt formalism (lines in Fig. 6). A Monte Carlo generated source with flow values from Ref. [14], zero lifetime, and with slope parameters for the energy spectra [14] served as input for this theoretical description. The simulated protons have passed through the experimental filter. With increasing incident energy the apparent source size decreases from 11 fm

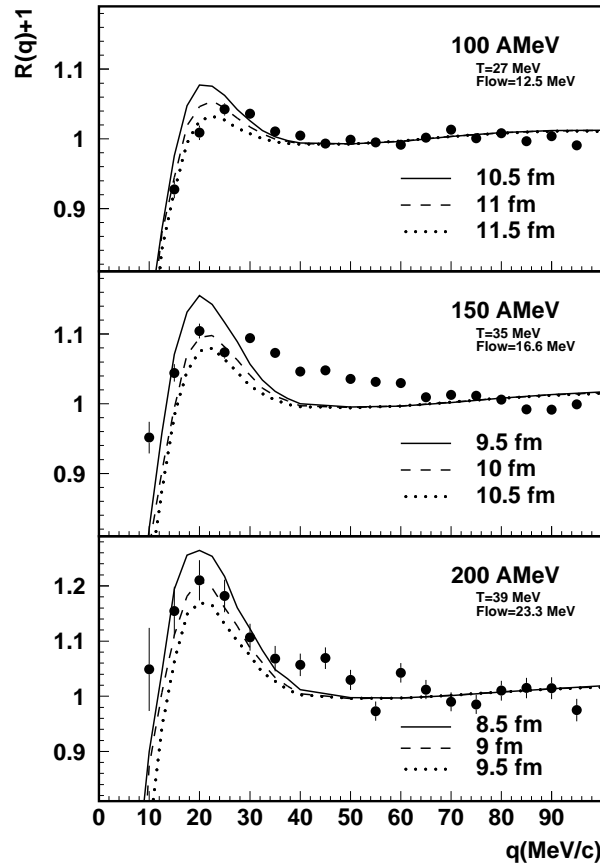


Figure 6: Proton-Proton correlation functions are shown for central collision at the indicated incident energies. Theoretical predictions (lines) indicate a shrinking apparent source size.

to 9 fm (hard sphere radius). These values are larger than the radius of the combined system of two Au nuclei at groundstate density. The systematical errors resulting from different methods of normalization are estimated to be about 0.5 fm.

In conclusion, we found for increasing beam energies of 50, 100, 150, and 200 AMeV Au+Au, for midrapidity fragments an increasing deviation between temperatures from double ratios of isotopic yields and temperatures extracted from excited state populations. This deviation can be explained by different freeze out conditions and different cooling of the nucleus. Then, it allows to investigate freeze out conditions for stable fragments and excited states. Source sizes from proton-proton correlation functions indicate a shrinking source size with increasing beam energy of 11 to 9 fm.

## References

- [1] J. Pochodzalla, T. Möhlenkamp, T. Rubehn, A. Schüttauf *et al.*, Phys. Rev. Lett. **75**, 1040 (1995)
- [2] G. Papp and W. Nörenberg, preprint GSI-95-30 (1995); Proceedings of the International Workshop XXII, Hirschegg, 1994, edited by H. Feldmeier and W. Nörenberg (GSI, Darmstadt, 1994) p. 87.
- [3] W. Trautmann *et al.*, contribution to these Proceedings.
- [4] S. Albergo, S. Costa, E. Costanzo and A. Rubbino, Il Nuovo Cimento **89A**, 1 (1985)
- [5] G. Röpke, L. Münchow and H. Schulz, Nuc. Phys. A **379**, 536 (1982); G. Röpke, M. Schmidt, L. Münchow and H. Schulz, Nuc. Phys. A **399**, 587 (1983); M. Schmidt, G. Röpke and H. Schulz, Ann. Phys. **202**, 57 (1990).
- [6] B. Tsang, Proceedings of the 1st Catania Relativistic Ion Studies: Critical Phenomena and Collective Observables, Acicastello, 1996.
- [7] F. Gulminelli *et al.*, contribution to these Proceedings.
- [8] J.B. Natowitz, K. Hagel, R. Wada, Z. Majka *et al.*, Phys. Rev. C **52**, R2322 (1995)
- [9] C. Schwarz, W.G. Gong, N. Carlin, C.K. Gelbke *et al.*, Phys. Rev. C **48**, 676 (1993)
- [10] G.J. Kunde, J. Pochodzalla, J. Aichelin, E. Berdermann *et al.*, Phys. Lett. B **272**, 202 (1991)
- [11] Z. Chen and C. K. Gelbke, Phys. Rev. C **38**, 2630 (1988)
- [12] H.J. Barz *et al.*, Phys. Lett. B **382**, 343 (1996)
- [13] H. Xi, GSI, Scientific Report 1995, 37
- [14] G. Poggi *et al.*, Nucl. Phys. A **586**, 755 (1995)
- [15] D. Hahn and H. Stöcker, Nucl. Phys. A **476** (1988) 718